

Thermal Annealing Effect on the Single Oscillator Energy and Dispersion Energy of Epitaxial Growth Bilyers of ZnS/ZnSe thin Films

Alaa A. Akl^{a,c}, Salah M.M. Salman^{b,d}

^aPhysics Department, Faculty of Science, El-Minia University, El-Minia, Egypt

^bPhysics Department, Faculty of Science, Helwan University, Ain-Helwan-Egypt

^cPhysics department, Faculty of Science, Ed Dawadmi, Shaqra University, Saudi Arabia

^dEducational Services, Qassim University, Ministry of High Education, Saudi Arabia

ABSTRACT

ZnS/ZnSe bilyers were preparing by stacking layers deposited on unheated glass substrates by thermal evaporation technique. We have studied the effect of thermal annealing of chalcogenide ZnS/ZnSe thin films on the dispersion parameters of refractive index. The refractive index, spectral dispersion of investigated was determined by Murmann's exact equation and analyzed. To calculate and discuss the dispersion parameters in the band gap region three different approaches were used (Cauchy, Sellmeier and Wemple–DiDomenico single-oscillator model). The obtained results showed that, the refractive index increased with increasing the annealing temperature and the dielectric properties have weak dependencies of annealing temperature. The average values of oscillator energy, E_0 and dispersion energy, E_d , were found to be 3.91 and 19.95eV. Also, the average values of the single resonant frequency ω_0 was estimated 7.89×10^{15} Hz. Furthermore, the optical parameters such as wavelength of single oscillator λ_0 , plasma frequency ω_p , and dielectric constant ϵ have been evaluated. Also, a value of carrier concentration based on Drude's theory was obtained in 1.75×10^{17} cm⁻³ for the as-deposited film and slight changes with annealing temperatures.

Keywords : Thin Films, Optical Dispersion, ZnSSe.

I. INTRODUCTION

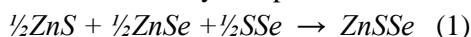
Recently, thin film of II-VI semiconductors have attracted them due to significant advances in the epitaxy growth techniques. Compared to relatively small band gap III-V structures, multi-layer composite the wider band-gap II-VI is more suitable for various optoelectronic devices that cover nearby infrared to the visible spectral range and ultraviolet [1-3]. ZnS-based II-VI wide-band-gap semiconductors, provides an opportunity to develop new optoelectronic devices that can combine high sensitivity in the ultraviolet (UV) region with minimal sensitivity in the visible region [4,5]. When ZnS combines with other materials such as ZnSe it produces stimulation and can be effective heterostructures such as ZnS/ZnSe systems. The manufacture of semiconductors thin film with layer thickness and highly controllable chemical composition was the result of recent advances in crystalline growth

techniques [6-8]. Optical constants include the valuable information for technological applications. Furthermore, the changes in refractive index are important for controlling the optical properties of ZnSSe. The investigation of optical constants, such as refractive index, extinction coefficient and dielectric constant of the ZnSSe, is important for the design of new materials. Optical constants include valuable information for technological applications. Moreover, changes in the refractive index are important for controlling the optical properties of ZnSSe. There are generally two sources of dispersion: dispersion of materials and waveguide dispersion. The dispersion of the material from the response depends on the frequency of the material to the waves. The refractive index, the dispersion of ZnSSe is important for optical applications, because optical properties are directly related to its structure. In this study, our study was completed by presenting the optical characteristic results obtained on the ZnSSe thin

films [9]. We are concerned that the heat treatment of bilayers ZnS/ZnSe that influence on the dispersion properties for optoelectronic applications. Some important optical absorption parameters such as single oscillator energy and dispersion energy E_o and E_d , dielectric constant ϵ , the ratio between number of charge carriers and effective mass N/m^* , wavelength of single oscillator λ_o , plasma frequency ω_p , and the single resonant frequency ω_o were evaluated.

II. THE EXPERIMENTAL WORK

ZnSSe films were prepared at room temperature by using stacked layers of ZnS and ZnSe of high purity (99.999%) followed by thermal annealing. The powder was first pressed at 100 kg/cm² into a pellet with 10mm in diameter to prevent scattering during deposition and then put inside small tungsten (W) boat inside the physical vapor deposition unit. The individual layer thicknesses were chosen to be in the ratios 1.0:1.48 to achieve a 1:1:1 stoichiometric ratio for Zn, S and Se, respectively. The total thickness of each sandwich was approximately 335nm (thickness of ZnS=135nm and ZnSe=200nm). Film thickness and deposition rate were monitored by a quartz crystal oscillator (Edwards Model FTM3). The annealing process was performed at different temperature, namely 250,300 and 350°C for 2h. Equation expected the chemical reactions to get the single phase of the ternary compound as follows [9];



Optical transmission and reflection spectra of investigating samples were measured by using a Shimadzu UV 3101 PC; UV-VIS-NIR double-beam spectrophotometer with the reflection attachment of V-N type (incident angle 5°). The optical tests in a wavelength range from 200 to 2500nm were carried out. In addition, optical characteristic measurements of the ZnSSe thin films such as the optical constants and dielectric functions were investigated using by the computation program [10].

3. Results and discussion

3.1. Optical properties

The spectral variation of transmittance and reflectance for as-deposited and after annealing of ZnSSe thin films are shown in Figs. (1&2). The obtained spectra of the films are characteristic of a typical semiconductor

material with good optical quality. It was observed that, the transmission and reflectance of all films have multiple interference fringes. The presence of interference fringes is due to multiple reflections at the substrate/film interface given the optical contrast, i.e. the different refractive index of ZnSSe and the substrate. In addition, the front edges of the transmission curves represent the intrinsic absorption of ZnSSe thin film. Moreover, that is an increase of annealing temperature decreases the transmittance, which means that the crystallization improved either the absorption. Also, it can be seen that the transmission spectrum has been divided into three special regions according to their transmission values: (i) the transparent region ($\lambda=1700-2500$ nm), where $T(\lambda)$ has higher value, (ii) the strong-absorption region, ($\lambda=200-750$ nm) and (iii) the absorption region, ($\lambda=750-1700$ nm). From this figure, the as-deposited film exhibits high transparencies in the visible and the NIR spectral regions. On the contrary, the annealing samples have lower transmittance claiming higher absorption.

3.2. Determination of refractive index

Refractive index is one of the fundamental properties of an optical material, because it is closely related to the electronic polarization of ions and the local field inside materials. The real n , and imaginary k , parts of the complex refractive index were determined from the corrected $T(\lambda)$ and $R(\lambda)$ using a developed computation program [10]. Both the transmittance and reflectance are given by [11]:

$$T(\lambda) = \left(\frac{I_{FG}}{I_G} \right) (1 - R_G), \quad (2)$$

where I_{FG} and I_G are the intensities of light passing through the film/glass substrate system and that passing through the reference glass, respectively, and R_G is the reflectance of the glass substrate, and

$$S = \left[\left(\frac{I_{FR}}{I_M} \right) R_M \left\{ 1 + (1 - R_G)^2 \right\} \right], \quad (3)$$

$$R(\lambda) = (S - T^2(\lambda)R_G), \quad (4)$$

where I_M is the intensity of light reflected from the reference mirror, I_{FR} is the intensity of light reflected from the sample and R_M is the mirror reflectance. In order to calculate the optical constants of the films at different wavelengths using the following equations:

$$Q = \sqrt{\frac{(1-R)^4}{4T^2} + R^2}, \quad (5)$$

$$\alpha = \frac{1}{t} \operatorname{Ln} \left[\frac{(1-R)^2}{2T} + Q \right], \quad (6)$$

$$n = \left(\frac{1+R}{1-R} \right) + \sqrt{\frac{4R}{(1-R)^2} - k^2}, \quad (7)$$

where α is the absorption coefficient and t is the film thickness. Figure 3 shows the spectral variation of the refractive index, n as a function of wavelength at different annealing temperature. It can be seen that, the behavior of refractive index, $n(\lambda)$ has a higher value at very low wavelength (strong absorption) for all samples. This is due to the equality between the frequency of incident electromagnetic radiation and the plasma frequency. Therefore, there is an anomalous dispersion of refractive index in the region of the plasma frequency. Furthermore, the maximum value of refractive index at very low wavelength, $\lambda = 200$ nm (strong-absorption region) was observed in all samples. This is referring to the equality between the frequencies of incident electromagnetic radiation with the frequency of vibration for electrons. This leads to the coupling of electrons in ZnSSe films with the oscillating of electric field. At longer wavelengths, $\lambda > 500$ nm, sharp decreasing of the refractive index of all patterns reaching to the lowest value at $\lambda \geq 900$ nm and then the n value remains slightly changed for the whole wavelength. In the NIR region, $\lambda \geq 1000$ nm, the $n(\lambda)$ values differ with annealing temperature then diverge remarkably in the visible region. These results are in good agreement with the data obtained by others [12-15] for like phase.

The extinction coefficient, $k(\lambda)$, of the obtained data was calculated using the simple relation [11]:

$$k = \frac{\alpha \lambda}{4\pi^2}, \quad (8)$$

It is observed from figure (4) that, the values of $k(\lambda)$ are markedly decreased as wavelength increases in the range from 200 to 800 nm. The large magnitude of $k(\lambda)$ value reaches to 0.35 ± 0.01 at $\lambda = 200$ nm. This value of $k(\lambda)$ was attributed to the fundamental band gap and the very low transmittance at short wavelength. The calculated values of $n(\lambda)$ and $k(\lambda)$ are in agreed with those obtained from like phase [12-15].

3.3. Dispersion behavior of refractive index

The dispersion of the refractive index can be explained by the application of electromagnetic theory to the molecular structure of the material. If the electromagnetic wave incident on the material causes the vibration of an atom or molecule, and the frequency of the atom is equal to the frequency of the incident wave, then, the resonance frequency is occurring. The obtained data of refractive index n can be analyzed to obtain the dispersion via three different methods. The first method was analyzed by using the Cauchy equation [16-18]:

$$n(\lambda) = a + \frac{b}{\lambda^2} + \frac{c}{\lambda^4} \quad (9)$$

The Cauchy parameters a , b and c represent characteristics of the material, and can be determined for a material by fitting the equation to measure refractive indices at known wavelengths. The values of the coefficient a are, in fact, refractive indices at infinite wavelength, (n_∞), that is static refractive indices. Although the above form of the function describes well the dispersion in a wider range of wavelengths, it is difficult to attribute clear physical meanings of their parameters [5]. For this reason the Cauchy equation has found application only as a means for the interpolation and extrapolation of experimental data, especially in the spectral regions close to the absorption edge. Usually, it is sufficient to use a two-term form of the relation [17,19]:

$$n(\lambda) = a + \frac{b}{\lambda^2} \quad (10)$$

Where the coefficients a and b are determined specifically for this form of the equation. Figure (5) represents the relationship between the refractive index and inverted of the square of the wavelength for all samples. The coefficients for the ZnSSe of the investigated samples are presented in Table 1.

The second method used for the analysis was the Sellmeier model, which relies on the assumption that the electrons of the condensed media oscillate also at the frequencies in the UV range. The Sellmeier Equation is especially suitable for the progression of refractive index in the wavelength range from the UV through the visible to the IR area (to 2.3 μm). The assumption that the dominant valence electrons in the

material oscillate at the very close (practically identical) frequencies, appeared to be fully justified. The model is then described by the following simplified equation [6]:

$$\frac{\lambda^2}{n^2 - 1} = \frac{\lambda^2}{A} - \frac{\lambda_o^2}{A} \quad (11)$$

where A is the total oscillator force, and λ_o is the wavelength corresponding to the eigenvalue of the oscillator frequency. In order to determine the coefficients A and λ_o the experimental data were linearized using the function of the form $\lambda^2/(n^2 - 1) = f(\lambda^2)$ (Figure 6), and the obtained coefficients (Table 1) served to calculate the static refractive index n_∞ ($n_\infty = \sqrt{1 + A}$). All the wavelengths λ_o relate to the near UV spectral range (from 206 to 263 nm), which is in agreement with the theoretical assumptions of this dispersion model. Static refractive indices n_∞ show the tendency of a mild increase with the change of annealing temperature. The results obtained by this method differ only a little from those obtained by the Cauchy analysis, the differences being less than 1.4%.

The third model used to analyze the refractive index, dispersion, derived from Wemple and Didomenico (WDD) single oscillator model [20,21], and most often applied for chalcogenide semiconductors. In this concept, the dispersion energy parameters E_d and E_o are introduced and the optical data could be described to an excellent approximation by the following expression:

$$(n^2 - 1)^{-1} = \frac{E_o}{E_d} + \frac{1}{E_o E_d} (h\nu)^2 \quad (12)$$

Where h is Planck's constant, ν is the frequency, $h\nu$ is the photon energy. The physical meaning of E_d is related to the average strength of interband optical transitions and is associated with the changes in the structural order of the material and the effective oscillator energy, while E_o can directly correlate with the optical energy gap by an empirical formula. E_o is considered as an average band gap, the so-called WDD band gap, and it corresponds to the distance between the 'centers of gravity' of the valence and the conduction bands: E_o is, therefore, related to the bond energy of the different chemical bonds present in the material. Experimental verification of the equation (12) can be obtained by plotting $(n^2 - 1)^{-1}$ versus $(h\nu)^2$ for

ZnSSe thin film (Figure 7). It is observed that the plot is linear over all the range from 3.0 to approximately 5.5 eV. The determination of E_o and E_d were estimated by a linear fitting using a plotting program. The estimated values for each dispersion energies are recorded in Table 2. The average values of E_o and E_d equal 3.843 and 19.208 eV, respectively. The oscillator energy E_o is an average energy gap and in a close approximation with the optical band gap E_g^d , in which, $E_o \approx 1.5 E_g^d$, as suggested by the WDD model [22-24]. The average value of the optical band gap from WDD model equals 2.563 eV. The refractive index n_o (at zero photon energy) is calculated by extrapolating the WDD dispersion equation to $h\nu \rightarrow 0$ (the static refractive index), which is defined by the infinite wavelength dielectric constant $\epsilon_\infty^{WDD} = n_o^2$, can be deduced from the dispersion relationship as follows:

$$n_o^2 = \left(1 + \frac{E_d}{E_o}\right) \quad (13)$$

The refractive index values of n_o ranges from 2.425 to 2.470, thus changing the value of the dielectric constant of ternary compound ZnSSe thin film from 5.881 to 6.101 (i.e. $\epsilon_\infty^{WDD} \approx 6.1$).

3.4. Determination of carrier concentration

The dispersion of refractive index, n , of the investigated ZnSSe films at different annealing temperature was analyzed by describing the contribution of free carriers and lattice vibration modes of the dispersion. The following equation shows the relation between the optical dielectric constant ϵ , wavelength λ and refractive index [22]:

$$\epsilon = n^2 = \epsilon_{\infty(t)} - \left(\frac{e^2}{4\pi c^2 \epsilon_o}\right) \left(\frac{N}{m^*}\right) \lambda^2 \quad (14)$$

where c is the velocity of the light, ϵ_o is the permittivity of free space (8.854×10^{-12} F/m), N is the free carrier concentration and m^* is the effective mass of charge carriers. The nature of the dispersion of n^2 as a function of wavelength (λ^2) for different laser powers is shown in (Figure 8).

It can be shown that the refractive index is an abnormal dispersion in the high frequency region. An increase in refractive index occurs and there is also an increase in

the absorption of electromagnetic radiation with increased frequency. Furthermore, the refractive index becomes large, when the frequency of radiation is repeated with the electron's characteristic frequency. Thus, there is no spread of electromagnetic radiation through the ZnSSe films. Figure 8 also shows that the dependence of n^2 is linear at longer wavelengths. The values of lattice high frequency dielectric constant $\epsilon_{\infty(1)}$ are determined from the intersection of the straight line with ($\lambda^2 = 0$). The values of $\epsilon_{\infty(1)}$ increase with increasing the laser powers. Table 2 shows the values of both $\epsilon_{\infty(1)}$ and the ration N/m^* of the investigated films at different temperature determined from the slopes of the line. The obtained values of the ratio N/m^* are in the range of (2.56×10^{47} – $1.57 \times 10^{47} \text{ cm}^{-3}\text{g}^{-1}$) with the change of temperature annealing. These results are in agreement with Al-Ghamdi et al. [25] for NiO thin films. Hutchines et al. [25] and El-Nahass et al. [26] found (N/m^*) for WO_3 , nickel phthalocyanine films, and also for V_2O_5 and $\alpha\text{-Fe}_2\text{O}_3$ thin films [27,28], in the same order. It is known that in the range of transparency, when the electron damping parameter $\gamma \ll \omega$,

$$n^2 = \epsilon_{\infty} - \frac{\omega_p^2}{\omega^2} \quad (15)$$

where ω_p is the plasma frequency $\omega_p^2 = e^2 N / \epsilon_o^2 m^*$, and ω is the incident light frequency [27, 28]. From the approximation of the linear part of the dependences $n^2(\lambda^2)$ of ZnSSe films annealed at different temperature (Fig.8) to $\lambda^2 = 0$ and $n^2 = 0$ the values of ϵ_{∞} and ω_p were listed in Table 3. Furthermore, it has been found that the band gap of the material is related to its refractive index approximately by $n^2 - 1 = N_c Z_a N_e / 6E_g$ [29,8]. Thus,

$$\beta = \frac{E_d}{6E_g (n_{\infty}^2 - 1)} \quad (16)$$

The results in Table 3 showed that at different temperatures, the values for β to vary from 0.317 to 0.427 (the average value is 0.369) were found.

This means that the bonds in the examined material (ZnSSe) have an ionic character [28,29] and indicate that for material containing the same ionic species, the β values slightly increase with the degree of crystallization and their crystallite size. This range value corresponds to values reported by other researchers [26,28].

Another way to calculate the concentration of free carrier is N_{opt} for ZnSSe films according to the classic Drud's theory. In theory, if the concentration of the free

carrier is high enough, the plasma resonance phenomenon takes place. The complex dielectric constant $\epsilon(\omega)$ is given by [22]:

$$\epsilon(\omega) = n^2 - k^2 = \epsilon_{\infty} - \frac{\omega_p^2}{\omega^2} = \epsilon_{\infty} - \frac{\lambda^2}{\lambda_p^2} \quad (17)$$

where ω_p and λ_p are the plasma resonance frequency and wavelength, respectively. If $\lambda < \lambda_p$, the complex dielectric constant is positive and solutions of the wave equation become oscillatory, which means that radiation can propagate. On the other hand, if $\lambda > \lambda_p$, solutions decay exponentially so that no radiation can propagate through the material. The plasma resonance ω_p is given by [22]:

$$\omega_p^2 = (4\pi N_{opt} e^2) (\epsilon_m \epsilon_o m_o)^{-1} \quad (18)$$

where N_{opt} is the free electron concentration, ϵ_m and ϵ_o represent the dielectric constant of the medium and free space, respectively, and m_o is the mass free carrier of the conduction band. The carrier concentration N_{opt} can be determined by using the relation:

$$N_{opt} = \frac{\epsilon_o \epsilon_{\infty} m_o \omega_p^2}{4\pi.e^2} \quad (19)$$

The calculated values of N_{opt} at different temperature are tabulated in Table 3. The average values of N_{opt} are equal to $1.749 \times 10^{17} \text{ cm}^{-3}$ for annealing temperature, which are in good agreement with the carrier concentration of other semiconductor [27,28,30].

III. Conclusions

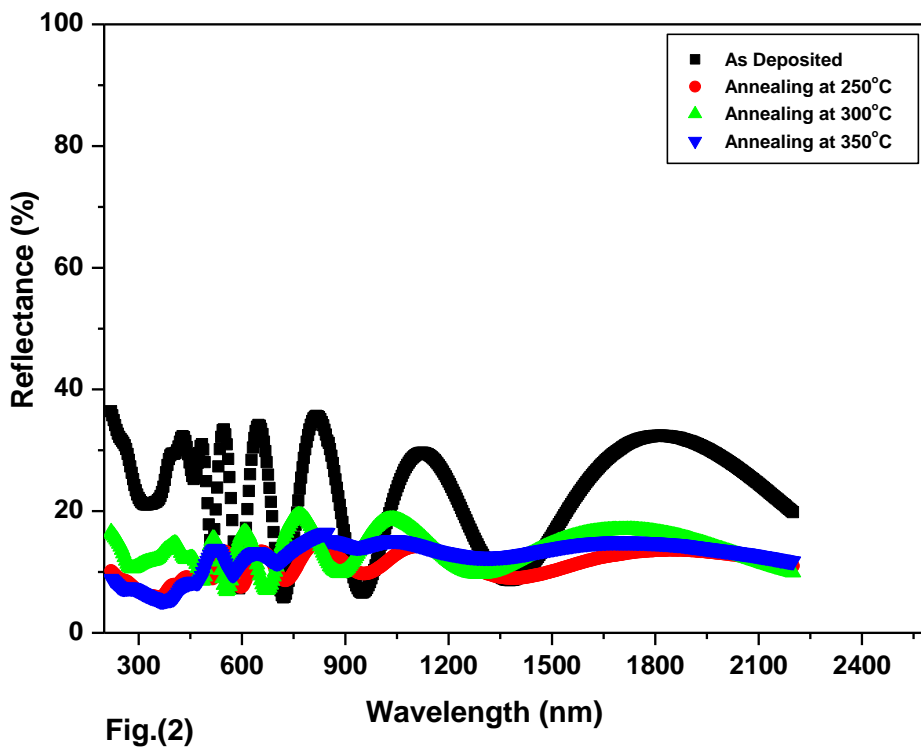
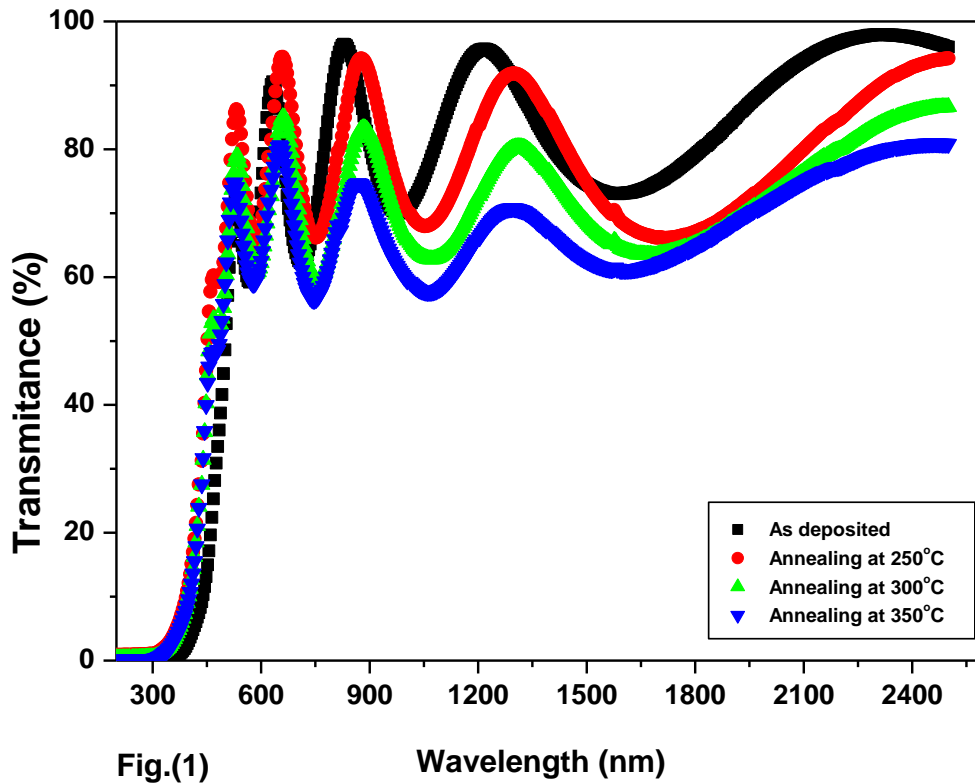
The effect of thermal annealing on the dispersion properties of the ternary compound ZnSSe thin films was studied. The refractive index changes slightly with thermal annealing temperature. Higher refractive index values were observed at a very low wavelength, $\lambda = 200\text{nm}$ in all samples. This is due to the coupling of the electrons in the ZnSSe films with the oscillating electric field. Also, the effect of annealing temperature on the dielectric constant, ϵ of the ternary compound was studied. The obtained values of $\epsilon_{\infty(1)}$ and $\epsilon_{\infty(2)}$ are slightly increased with increasing temperature. The values obtained of N/m^* are within (2.56 - 1.57) $\times 10^{47} \text{ cm}^{-3}.\text{g}^{-1}$ with varying temperature. The values of E_o and E_d increase as the annealing temperature increases,

and this can be attributed to the increase in the number of scattering centers due to the dissolving of zinc atoms in the film matrix. In addition, an experimental factor between a single oscillator energy E_o and the lowest direct-range gap $E_g(D)$ was found to be 2.52eV for ZnSSe at a different temperature. Furthermore, the values of N_{opt} based on Drude's theory are in the range of 2.33×10^{17} to $1.43 \times 10^{17} \text{cm}^{-3}$ with the changing the annealing temperature.

IV. REFERENCES

- [1]. Y. K. Liu, J. A. Zapien, Y. Y. Shan, C. Y. Geng, C. S. Lee, S. T. Lee, *Adv. Mater.* 17 (2005) 1372.
- [2]. P. X. Gao, Y. Ding, Z. L. Wang, *Nano Lett.* 3 (2003) 1315.
- [3]. A. L. Pan, H. Yang, R. B. Liu, R. C. Yu, B. S. Zou, Z. L. Wang, *J. Am. Chem. Soc.* 127 (2005) 15692.
- [4]. F. Qian, S. Gradecak, Y. Li, C. Y. Wen, C. M. Lieber, *Nano. Lett.* 5 (2005) 2287.
- [5]. M. S. Arnold, P. Avouris, Z. W. Pan, Z. L. Wang, *J. Phys. Chem. B* 107(2003) 659
- [6]. P. Nguyen, H. T. Ng, T. Yamada, M. K. Smith, J. Li, J. Han, M. Meyyappan, *Nano Lett.* 4 (4) (2004) 651.
- [7]. J. Xiang, W. Lu, Y. Hu, Y. Wu, H. Yan, C. M. Lieber, *Nature (London)* 441 (2006) 489.
- [8]. Y. Cui, Q. Wei, H. Park, C. M. Lieber, *Science* 293 (2001) 1289.
- [9]. Alaa. A. Akl, S. A. Aly, H. Howari ; *Chalcogenide Letters*, Vol. 13, No. 6, (2016) 299-306.
- [10]. M. M. El-Nahass, *J. Mater. Sci.* 27 (1992), 6597
- [11]. M. M. El-Nahass, A. A. M. Farag and A. A. Atta, *Synth. Mat.* 159 (2009), 589.
- [12]. S. A. Mahmoud, S. A. Aly, M. Abdel-Rahman, K. Abdel-Hady, *Physica B* 293 (2000) 125.
- [13]. O. S. Heavens, *Optical Properties of Thin Films*, Dover, New York, (1965).
- [14]. K. M. M. Abo-Hassan, M. R. Muhamad, S. Radhakrishna, *Thin Solid Films* 491 (2005) 117.
- [15]. C. Mehta, G. S. S. Saini, J. M. Abbas, S. K. Tripathi, *Applied Surface Science* 256 (2009) 608.
- [16]. G. I. Rusu, M. Diciu, C. Prîrghie, E. M. Popa, *Applied Surface Science* 253 (2007) 9500.
- [17]. M. B. El-Den, M. M. El-Nahass, *J. Opt. Laser Technol.* 35 (2003) 335
- [18]. E. Santhi, V. Dutta, A. Banerjee, K. L. Chopra, *J. Appl. Phys.* 51 (1980) 6243.
- [19]. F. Skuban, S. R. Lukic, D. M. Petrovic, I. O. Guth, *J. of non-crystalline solids*, 355 (2009) 2059.
- [20]. A. K. S. Aqili, A. Maqsood, Z. Ali, *Appl. Surf. Sci.* 191 (2002) 280.
- [21]. R. Swanepoel, *J. Phys. E: Sci. Instrum.* 17 (1984) 869.
- [22]. V. Darakchieva, M. Baleva, M. Surtchey, E. Goranova, *Phys. Rev. B* 62 (2000) 13057
- [23]. M. B. El-Den, M. M. El-Nahass, *J. Opt. Laser Technol.* 35 (2003) 335
- [24]. A. A. Al-Ghamdi, W. E. Mahmoud, S. J. Yaghmour, F. M. Al-Marzouki, *J. Alloys and Compounds* 486 (2009) 9.
- [25]. M. G. Hutchins, O. Abu-Alkhair, M. M. El-Nahass, K. Abdel-Hady; *Materials Chemistry and Physics* 98 (2006) 401.
- [26]. M. M. El-Nahass, A. M. Farag, K. F. Abd El-Rahman, A. A. A. Darwish, *Optics & Laser Technology* 37 (2005) 513.
- [27]. A. A. Akl, *Applied Surface Science* 256 (2010) 7496.
- [28]. A. A. Akl, *Journal of Physics and Chemistry of Solids* 71 (2010) 223.
- [29]. J. J Pankove, *Optical Processes in Semiconductors*, Prentice-Hall, Englewood Cliffs, NJ, 1971
- [30]. A. A. Akl, *J. Phys. Chem. Solids* 71 (2010) 223.

All figures for ZnS/ZnSe bilayer thin films



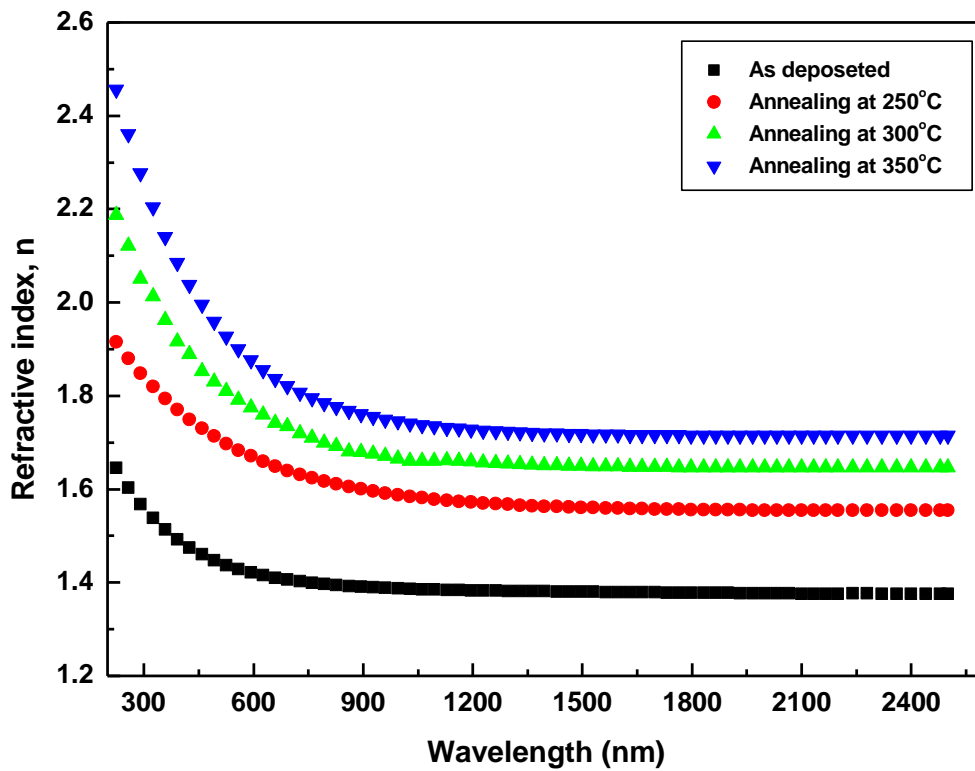


Fig.(3)

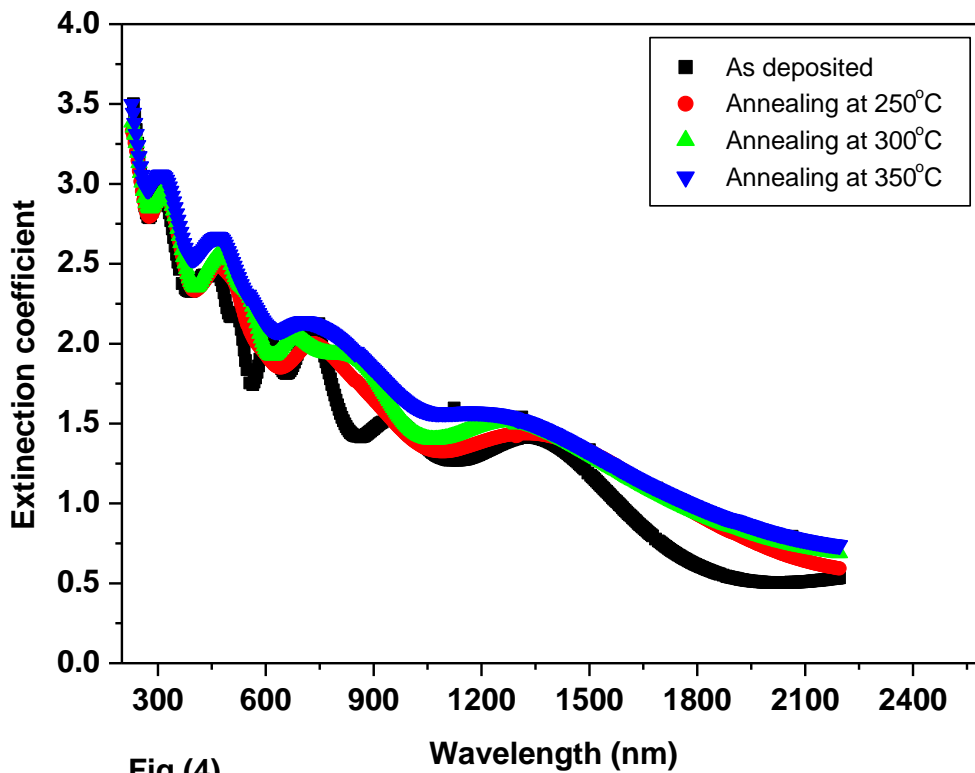


Fig.(4)

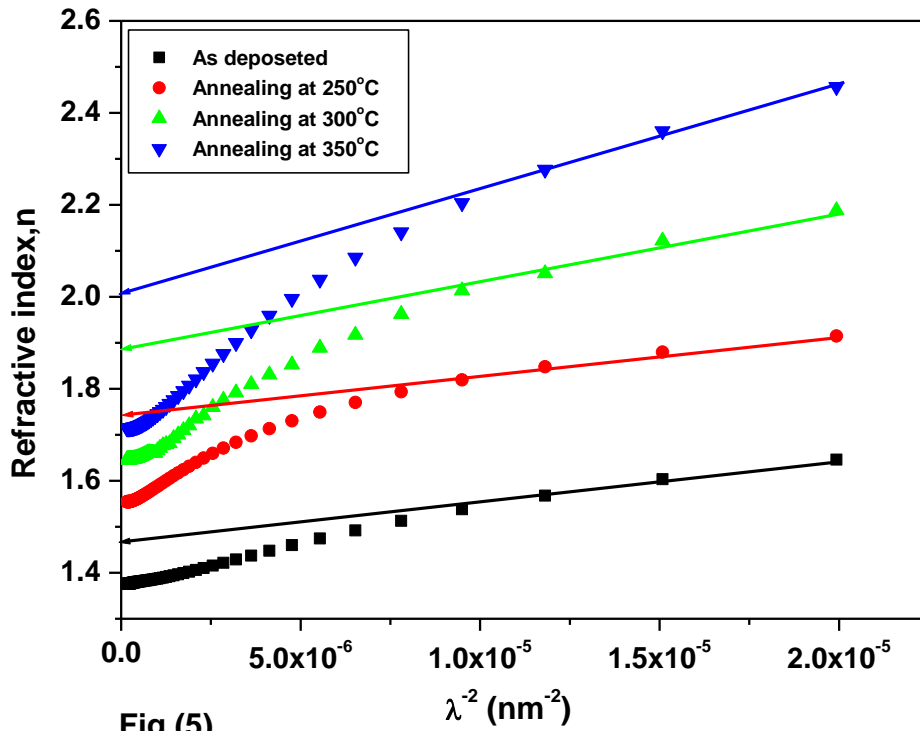


Fig.(5)

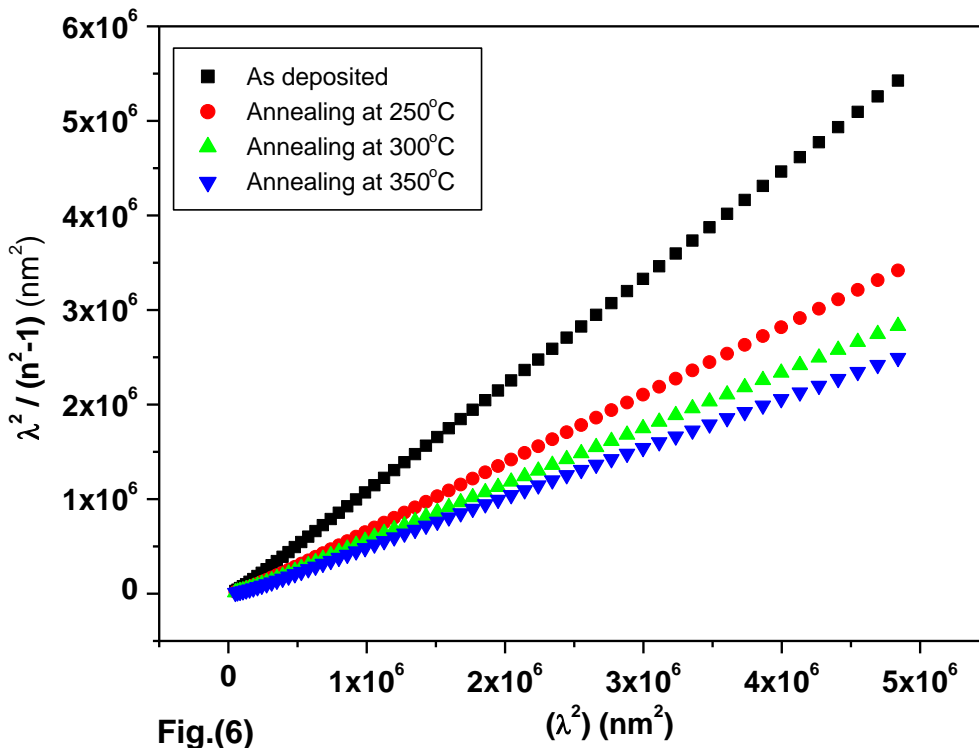


Fig.(6)

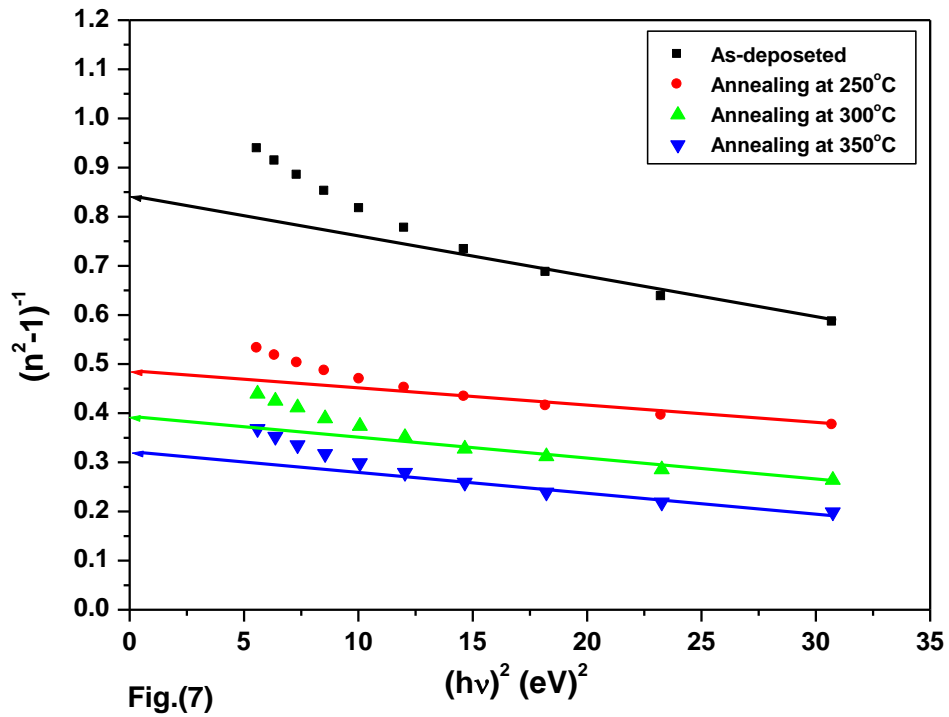


Fig.(7)

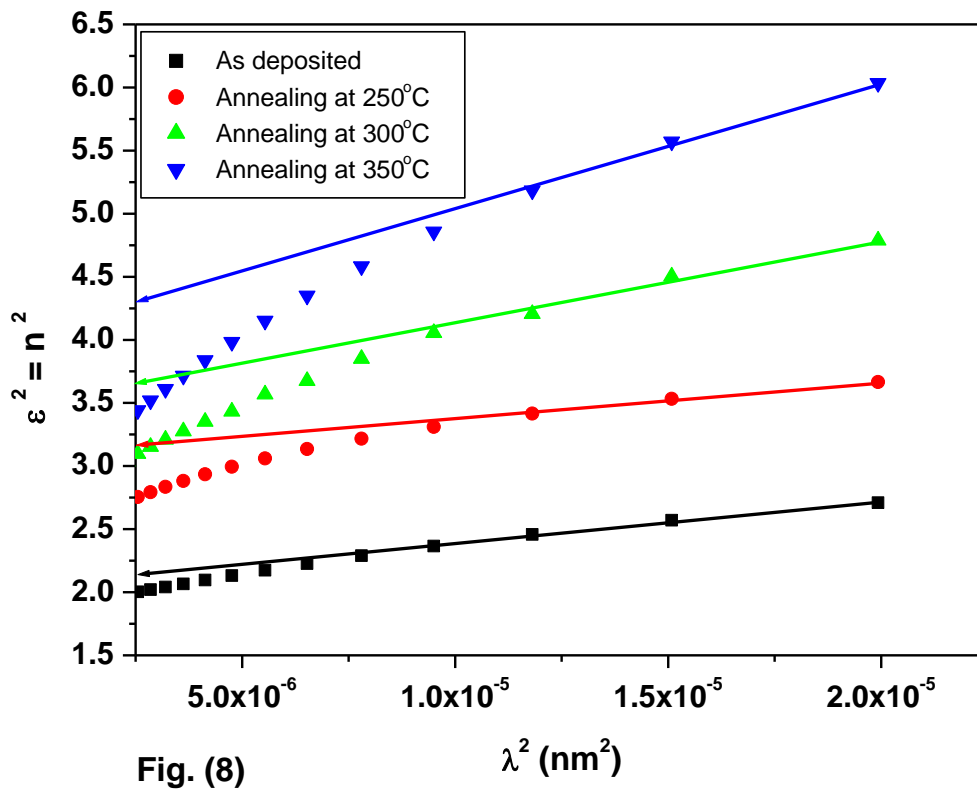


Fig. (8)

Table 1: Parameters of dispersion analysis determined in the different approaches for the ZnSSe thin films .

Sample condition	Cauchy			Sellmeier			Wemple-DiDomenico			E_g
	$a=n_\infty$	$b(10^5 nm^2)$	$c(10^{10} nm^4)$	A	$\lambda_o(nm)$	n_∞	$E_o(eV)$	$E_d(eV)$	n_∞	
As deposited	2.414	1.206	6.297	5.246	206	2.499	3.78	18.45	2.425	2.52
Annealing at 250°C	2.423	1.230	6.870	5.384	239	2.527	3.82	18.78	2.432	2.55
Annealing at 300°C	2.442	2.192	6.963	5.542	256	2.558	3.86	19.65	2.467	2.57
Annealing at 350°C	2.458	3.033	7.042	5.686	263	2.586	3.91	19.95	2.470	2.61

Table 2: The calculation of dispersion characteristics for ZnSSe thin film annealed at different temperatures.

Sample condition	ϵ_L		N/m* ($cm^{-3} g^{-1}$) ($\pm 3.7 \times 10^{-2}$)	λ_o (nm) ($\pm 2.1 \times 10^{-3}$)	E_d (eV) ($\pm 3.2 \times 10^{-4}$)	E_o (eV) ($\pm 5.6 \times 10^{-4}$)	n_∞ ($\pm 2.7 \times 10^{-4}$)
	$\epsilon_{\infty(1)}$ ($\pm 4.3 \times 10^{-4}$)	$\epsilon_{\infty(2)}$ ($\pm 6.7 \times 10^{-4}$)					
As-deposited	2.242	5.881	2.561×10^{47}	206	18.453	3.782	2.425
Annealing at 250°C	3.225	5.915	1.899×10^{47}	239	18.784	3.825	2.432
Annealing at 300°C	3.863	6.086	1.664×10^{47}	256	19.652	3.864	2.467
Annealing at 350°C	4.308	6.101	1.574×10^{47}	263	19.951	3.910	2.470